Magnetic Properties of Some Triangular Trinuclear Complexes of $[Ru_2M(\mu\text{-}CH_3COO)_6(\mu_3\text{-}O)(py)_3]^{n+}$ with a Paramagnetic Ion M

Hanako Kobayashi,* Norikiyo Uryû,† Iwao Mogi,†† Ryo Miyamoto,††† Yasunori Ohba,†††† Masamoto Iwaizumi,†††† Yoichi Sasaki,††††† Akihiro Ohto,§§ Masaaki Suwabe,§ and Tasuku Ito§§

Department of Physics, Toin University of Yokohama, Yokohama 225

†Faculty of Engineering, Nagasaki University, Nagasaki 852

††Institute of Materials Research, Tohoku University, Sendai 980-77

†††Faculty of Science, Hirosaki University, Hirosaki 036

††††Institute of Chemical Reaction Science, Tohoku University, Sendai 980-77

†††††Graduate School of Science, Hokkaido University, Sapporo 060

§Fuji Xerox Co.Ltd., Ebina 243-04

§§Graduate School of Science, Tohoku University, Sendai 980-77

(Received April 26, 1996)

Magnetic susceptibilities and electron paramagnetic resonances (EPRs) of coordination compounds of triangular trinuclear $[Ru_2M(\mu\text{-}CH_3COO)_6(\mu_3\text{-}O)(py)_3]^{n+}$, M = Mn(II), Fe(III), Cr(III), Ni(II), or Co(II) ions, were observed. The results were analysed by the spin vector model. Effective Bohr magneton numbers showed that the main superexchange interaction within each cluster was of the order of $J/k = -300$ K. This was considered to be working through μ_3-O. Together with some weaker superexchange interactions through μ-CH_3COO paths, fittings with the susceptibilities of the model were tried. EPR signals at temperatures of a few K were characteristic of each M ion. M = Mn(II) and M = Fe(III) were at high spin states of $S = 5/2$ and M = Co(II) was at a low spin state of $S = 1/2$. Temperature dependences of EPR signals are discussed.

Since the basis for the understanding of the magnetic properties of molecules was first established by J. H. Van Vleck[1] in 1932, special attention to the magnetism of molecules has been given in Ref. 2 in 1973 on the loss of orbital magnetic moments by their low symmetry and strong crystal fields. In Ref. 3 published in 1976, W. E. Hatfield introduced in the "Properties of magnetically condensed compounds (compounds with spin exchange)" Kambe's treatment of trimers,[4] which had been published in 1950. Kambe made clear fitting calculations with a model used the spin vector method to the experimental results of magnetic susceptibilities of trimers of 3d ions. As a result, Kambe showed that the orbital magnetic moment is lost in the trimers. Following Refs. 2 and 3, Refs. 5 and 6 were published for many papers on magnetic properties of magnetic dimers, trimers, tetramers, etc. These papers are mostly on the clusters with homologous paramagnetic metal ions and their magnetic properties were explained by the orthodox vector model.

In Ref. 7, measured magnetic properties of symmetric $[Ru_3(\mu\text{-}CH_3COO)_6(\mu_3\text{-}O)(py)_3]ClO_4$, were reported. Their coordinations with μ-CH_3COO's, μ_3-O, and py's in the cluster are the same as those of the present samples. A projection of the structure is shown in Fig. 1a, following Ref. 8. In the analysis of the magnetic susceptibilities at temperatures between 2 K and room temperature by the localized spin vector model, we tried to consider the strong exchange interactions through μ_3-O paths and the weak exchange interactions through six μ-CH_3COO paths. The fitting calculation showed that there is working an exchange interaction of $J = [-69.5\ cm^{-1}$ (non-rationalized CGSemu)], that is, $J/k = -99.97$ K between each two Ru ions.

In Ref. 9, magnetic properties of $[Ru_2M(\mu\text{-}CH_3COO)_6(\mu_3\text{-}O)(py)_3]^{n+}$, (M = Zn(II), Mg(II), or Ru(II); $n = 0$, or Rh(III); $n = 1$), salts were analyzed. Their coordinations in the clusters also are the same as those of the present samples. These samples are mixed clusters of two paramagnetic 4d ions and a diamagnetic 3d ion or a 4d ion. They were considered to be magnetic dimers, but temperature dependences of the magnetic susceptibilities were much different with that of ordinary dimers. Their fitting calculations by the spin vector method readily showed that these dimers are constituted with very weak antiferromagnetic exchange interactions of $J_1/k = -1.4$——-6.5 K, antiferromagnetic exchange interactions of $J_2/k = -40$——-110 K and strong antiferromagnetic exchange interactions of $J_3/k = -500$——-900 K with respective probabilities. Thus the antiferromagnetic

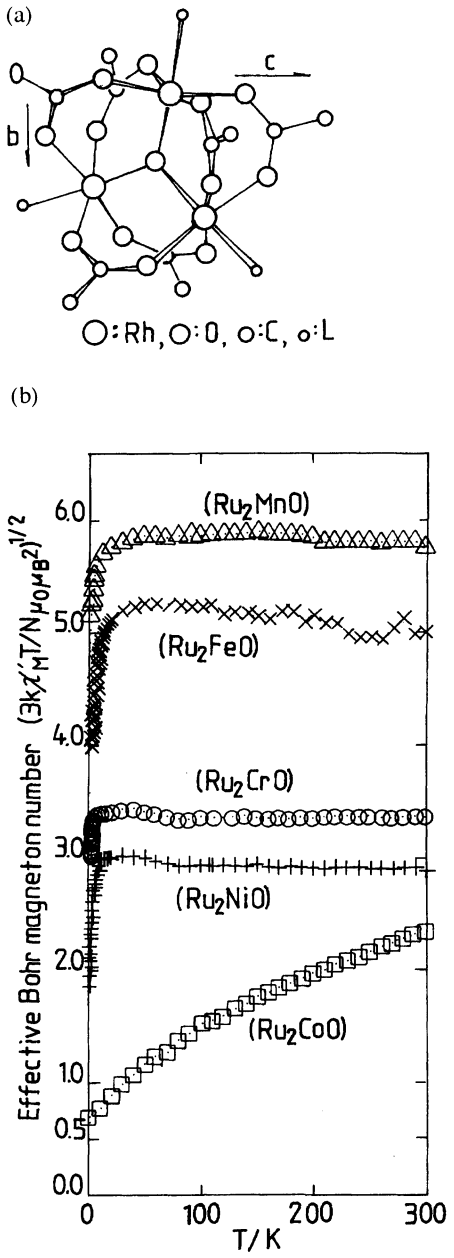

Fig. 1. (a) A projection of the structure of $[Rh_3(\mu\text{-}CH_3COO)_6(\mu_3\text{-}O)L_3]^+$ ion along the a-axis quoted from Ref. 2. (b) Effective Bohr magneton numbers, μ_{eff}'s, of all the samples as a function of temperatures. As seen in the text, J_1/k, α_1, $P(J_1,\alpha_1)$, J_2/k, α_2, $P(J_2,\alpha_2)$, and g-value of the lowest exchange interaction energy level of each sample are: (Ru_2MnO); −300 K, −1, 0.425, −0.6 K, 4, 0.575, and $g=2.18$, (Ru_2FeO); −300 K, −1, 0.480—0.550, −0.8 K, −1, 0.520—0.450, and $g=1.92$, (Ru_2CrO); −450 K, −1, 0.520, −0.3 K, −2, 0.480, and $g=1.94$, (Ru_2NiO); −300 K, 1.995, 0.745, −140 K, 3.00, 0.255, and $g=2.34$, and (Ru_2CoO); −300 K, −2, 0.839, −50 K, −2, 0.161, and $g=1.15$.

exchange interactions were assigned as follows: the J_3 acts through μ_3-O, the J_2 through two μ-CH_3COO paths between two Ru(III), and the very weak J_1 acts through –(double-μ-CH_3COO)–M–(double-μ-CH_3COO)– path. The mixing of two 4d ions and a 3d ion might cause fairly large magnetic distortions in the clusters.

Succeeding Ref. 9, triangular trinuclear clusters $[Ru_2M(\mu\text{-}CH_3COO)_6(\mu_3\text{-}O)(py)_3]^{n+}$, (M = Mn(II), Fe(III), Cr(III), Ni(II), or Co(II)), were synthesized. Their magnetic properties have shown characteristic of the M ion in each cluster, though observed magnetic susceptibilities and EPRs on powder could not give as much information as the single crystal does. The graphs, Fig. 1b, of effective Bohr magneton numbers[10] versus temperatures evidently showed that there were working a strong antiferromagnetic exchange interaction and a very weak antiferromagnetic exchange interaction in each cluster. Following Kambe's spin vector method[4] the Hamiltonian $\mathscr{H}=-2J[(S_1S_2)+(S_3S_1)+\alpha(S_2S_3)]$ was rewritten as $\mathscr{H}=\sum_{n=1,2}P(J_n,\alpha_n)[-2J_n\{(S_1S_2)+(S_3S_1)+\alpha_n(S_2S_3)\}]$, though for the Zeeman effect experimental g-values were used following Ref. 11. Here S_1 is the spin of M ion and S_2 and S_3 are the spins of Ru(III) ions. Between S_1 and S_2, and S_3 and S_1, exchange interactions J_n's are acting and between S_2 and S_3, an exchange interaction α_nJ_n is working. Dark colours of the samples might indicate that there are some delocalizations of electrons, and as a result of the analysis, it has been shown that the spins in the present clusters of 4d and 3d ions with structures like the present samples should be treated as spins in the molecular orbitals.

Abbreviations, (Ru_2MnO) for $[Ru_2Mn(\mu\text{-}CH_3COO)_6(\mu_3\text{-}O)(py)_3]\cdot py$, hexakis($\mu$-acetato-$\varkappa O:\varkappa O'$)-$\mu_3$-oxo-tris(pyridine)-triangulo-manganese(II) diruthenium(III)–pyridine-(1/1), (Ru_2FeO) for $[Ru_2Fe(\mu\text{-}CH_3COO)_6(\mu_3\text{-}O)(py)_3]PF_6$, hexakis($\mu$-acetato-$\varkappa O:\varkappa O'$)-$\mu_3$-oxo-tris(pyridine)-triangulo-iron(III) diruthenium(III) hexafluoro-phosphate, (Ru_2CrO) for $[Ru_2Cr(\mu\text{-}CH_3COO)_6(\mu_3\text{-}O)(py)_3]PF_6$, hexakis($\mu$-acetato-$\varkappa O:\varkappa O'$)-$\mu_3$-oxo-tris(pyridine)-triangulo-chromium(III) diruthenium(III) hexafluorophosphate, (Ru_2NiO) for $[Ru_2Ni(\mu\text{-}CH_3COO)_6(\mu_3\text{-}O)(py)_3]\cdot py$, hexakis($\mu$-acetato-$\varkappa O:\varkappa O'$)-$\mu_3$-oxo-tris(pyridine)-triangulo-nickel(II) diruthenium(III)–pyridine(1/1), and (Ru_2CoO) for $[Ru_2Co(\mu\text{-}CH_3COO)_6(\mu_3\text{-}O)(py)_3]\cdot py$, hexakis($\mu$-acetato-$\varkappa O:\varkappa O'$)-$\mu_3$-oxo-tris(pyridine)-triangulo-cobalt(II) diruthenium(III)–pyridine(1/1), are used in the following.

Experimental

Preparations. The preparations of $[Ru_2Mn(\mu\text{-}CH_3COO)_6(\mu_3\text{-}O)(py)_3]\cdot py$; ($Ru_2MnO$), $[Ru_2Ni(\mu\text{-}CH_3COO)_6(\mu_3\text{-}O)(py)_3]\cdot py$; ($Ru_2NiO$), $[Ru_2Ni(\mu\text{-}CH_3COO)_6(\mu_3\text{-}O)(py)_3]\cdot CH_2Cl_2$, and $[Ru_2Co(\mu\text{-}CH_3COO)_6(\mu_3\text{-}O)(py)_3]\cdot py$; ($Ru_2CoO$) followed the method of Ref. 12. $[Ru_2Cr(\mu\text{-}CH_3COO)_6(\mu_3\text{-}O)(py)_3)]PF_6$; ($Ru_2CrO$) and $[Ru_2Fe(\mu\text{-}CH_3COO)_6(\mu_3\text{-}O)(py)_3]PF_6$; ($Ru_2FeO$) were prepared by methods in Ref. 13.

Magnetic Susceptibility. The magnetic susceptibilities of (Ru_2MnO), (Ru_2FeO), (Ru_2CrO), (Ru_2NiO), and (Ru_2CoO) in the temperature region between near 2 K and room temperature were measured using a flux meter with a superconducting quantum interference device (SQUID) sensor of Quantum Design Inc. CA, U.S.A. Susceptibilities were measured under applied magnetic fields of 4000×10^2 A m^{-1}. Details of the measurements were the same as those in Ref. 9.

Magnetizations were also measured using the same fluxmeter

at 10 K to the applied magnetic field of 43770×10^2 A m^{-1}. No samples showed ferromagnetism or weak ferromagnetism.

EPR. The spectra of EPR of X-band, and of Q-band in a few cases, as a function of the flux density were measured at several temperatures in the region from near 6 K to near 100 K using the apparatus E102 or E231 of the Varian Instrument Division (Palo Alto, CA, U.S.A.) and in the region from about 100 K to room temperature using the apparatus of JEOL (Japan) at the X-band.

Units. Some values calculated in non-rationalized CGS emu[14] are snown in brackets [ ].

Results and Discussion

The observed effective Bohr magneton numbers,[10] μ_{eff}'s, showed common properties, that is, the magnitudes of μ_{eff}'s are much smaller than the case of the cluster with very weak exchange interaction. The μ_{eff} is $(3k\chi'_M T/N\mu_O\mu_B^2)^{1/2}$, where k means Boltzmann const.; N, Avogadro no.; μ_B, Bohr magneton; and μ_O, permeability of a vacuum. The χ'_M is corrected for χ_{dia} and χ_{TIP}. If the exchange interactions are very weak, μ_{eff}'s of (Ru_2MnO), (Ru_2FeO), (Ru_2CrO), (Ru_2NiO), and (Ru_2CoO) should be near 10.2, 10.2, 8.07, 7.03, and 5.93 respectively. The observed μ_{eff}'s of all the samples as seen in Fig. 1b showed that some strong antiferromagnetic exchange interactions are working in the clusters. On the other hand, the observed temperature dependences of μ_{eff}'s, except (Ru_2CoO), suddenly decreased at very low temperatures from almost constant values at higher temperatures respectively. This is characteristic of the weak antiferromagnetic exchange interaction cluster (as shown in Fig. 3a). To explain these observed properties, strong superexchange interaction paths which used μ_3-O bridges and weak superexchange interaction paths through acetato-bridges were introduced in the consideration.

$[Ru_2Mn(\mu\text{-}CH_3COO)_6(\mu_3\text{-}O)(py)_3]\cdot py$. The molar magnetic susceptibility of dark violet powder of (Ru_2MnO), corrected for the diamagnetic molar susceptibility χ_{dia}[15]$=-5.9650\times10^{-9}$ m^3 [-475.00×10^{-6} cm^3] is plotted in Fig. 2 as a function of temperature. From its plot as a function of reciprocal temperatures, experimental $\chi_{TIPexp}=1.26\times10^{-9}$ m^3 [100×10^{-6} cm^3] was obtained. The effective Bohr magneton numbers are plotted with triangle marks as a function of temperature in Fig. 3. The values at room temperatures are about 5.8. In Fig. 1b, effective Bohr magneton numbers

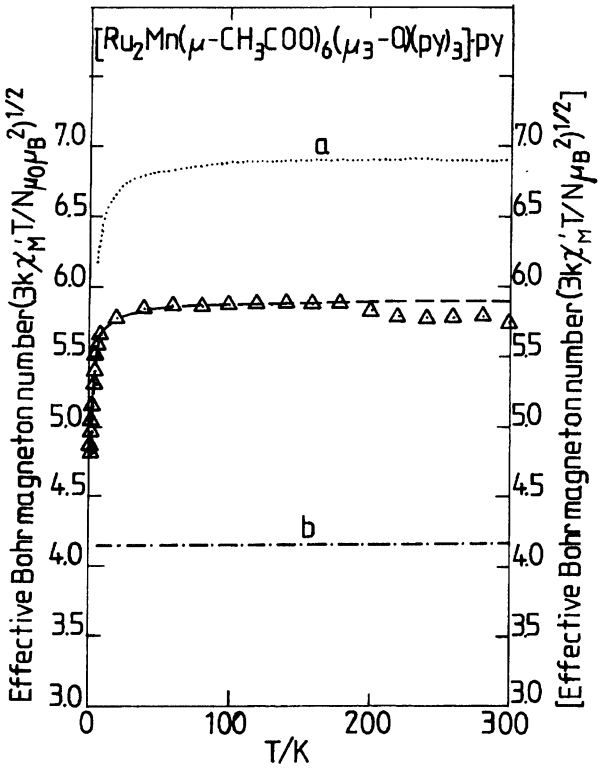

Fig. 3. Effective Bohr magneton numbers, μ_{eff}'s, of $[Ru_2Mn(\mu\text{-}CH_3COO)_6(\mu_3\text{-}O)(py)_3]\cdot py$ as a function of temperatures. △; data. χ'_M's are corrected for χ_{TIPexp} and χ_{dia}. ---; calculated values with $J_1/k=-300$ K, $\alpha_1=-1$, $P(J_1,\alpha_1)=0.425$, $J_2/k=-0.6$ K, $\alpha_2=-4$, and $P(J_2,\alpha_2)=0.575$. $g_{Mn}=2.18$ and $g_{Ru}=2.09$. a: ····; calculated values with $J/k=-0.6$ K, $\alpha=4$, $P(J,\alpha)=1$, $g_{Mn}=2.18$, and $g_{Ru}=2.09$. b: -·-; calculated values with $J/k=-300$ K, $\alpha=-1$, $P(J,\alpha)=1$, $g_{Mn}=2.18$ and $g_{Ru}=2.09$.

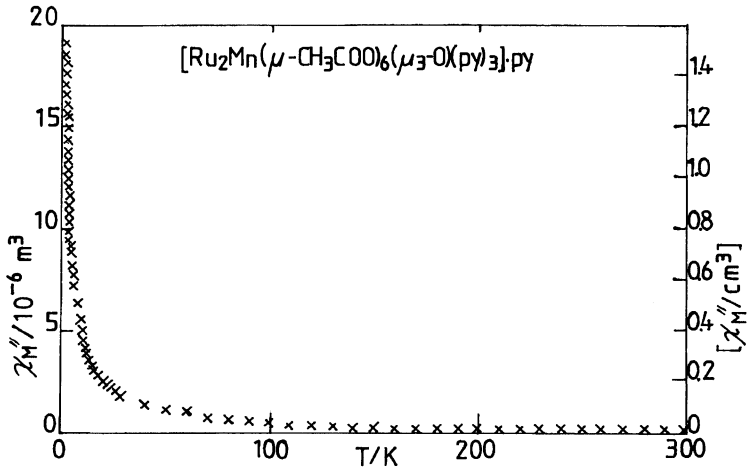

Fig. 2. The molar magnetic susceptibility of $[Ru_2Mn(\mu\text{-}CH_3COO)_6(\mu_3\text{-}O)(py)_3]\cdot py$ as a function of temperatures. χ''_M's are corrected for χ_{dia}.

of all the samples are shown as functions of temperatures, where Mn(II) in (Ru_2MnO) has a possibility to be in the high spin state of $S=5/2$ in comparison with others.

The EPR spectrum of powder of (Ru_2MnO) observed by X-band (9.1675 GHz) at 6.6 K is shown in Fig. 4a. The signal pattern is characteristic of the high spin of Mn(II). This signal was considered to be mainly due to Mn(II), as will be shown later. The experimental $g_{\perp exp}$'s were seen at 0.0852 T [843 0e] and 0.1197 T [1185 0e], whose averaged value was $g_{\perp exp}=6.77$, and $g_{\parallel exp}=1.97$ was observed at 0.3350 T [3316 0e] at 10—140 K. The resonances with Q-band (35.061 GHz) were observed at 103—133 K; these gave broad signals of $g_{\perp exp}=6.20$ and $g_{\perp exp}=5.60$, giving an averaged value of $g_{\perp exp}=5.90$. Using these EPR data obtained on powder at 103—133 K, $g_{\perp}=2.27$ and $g_{\parallel}=1.97$, and $|D|=0.0086$ m^{-1} [0.86 cm^{-1}] were approximately obtained following Ref. 16. That is, $\gamma = g_{\perp exp(X-band)}/g_{\perp exp(Q-band)}$ and $\delta=(H_{(X-band)}/H_{(Q-band)})^2$ are put, $g_{\perp}=g_{\perp exp(X-band)}(\gamma-\delta)/3\gamma(1-\delta)$, $g_{\parallel}=g_{\parallel exp}$, and $|2D|=g_{\perp}\mu_B\cdot\{2(\gamma H_{(Q-band)}{}^2-H_{(X-band)}{}^2)/(\gamma-1)\}^{1/2}$ were calculated(H; the applied magnetic field), where only the axial anisotropy of the ligand field was considered. The averaged g-value of Mn(II), $g_{Mn}=2.18$ and that of Ru(III), $g_{Ru}=2.09$ were used in the fittings of the molar magnetic susceptibility. The g-value of Ru(III) could not be determined from the EPR data of the present sample at low temperatures. The $g_{Ru}=2.09$ is a value obtained in the EPR of [$Ru_2Zn(\mu$-$CH_3COO)_6(\mu_3$-O)(py)$_3$]·CH_2Cl_2, (Ru_2ZnO),[9] which was almost temperature independent, showing that the orbital angular momentum of Ru(III) ion is almost lost. Since in all the samples of Refs. 7 and 9, Ru(III) was in the low spin state of $S=1/2$, the low spin state of Ru(III) is also assumed in this report.

Following Kambe's spin vector model[4,11] spin states $W(S',S^*)$, where $S'=S_1+S_2+S_3$, $S^*=S_2+S_3$, and S_1; spin of Mn(II), are $W_a(7/2,1)$, $W_b(5/2,1)$, $W_c(3/2,1)$, and $W_d(5/2,0)$. The lowest spin level of (Ru_2MnO), if antiferromagnetic exchange interactions are assumed, is of W_d. Namely a spin of Mn(II) is $S_1=5/2$ and spins of two Ru(III) ions are $S_2+S_3=0$, then the averaged g-value obtained by EPR at 6.6 K has a possibility of the signal of Mn(II). The molar magnetic susceptibility,[4,11] was calculated as follows.

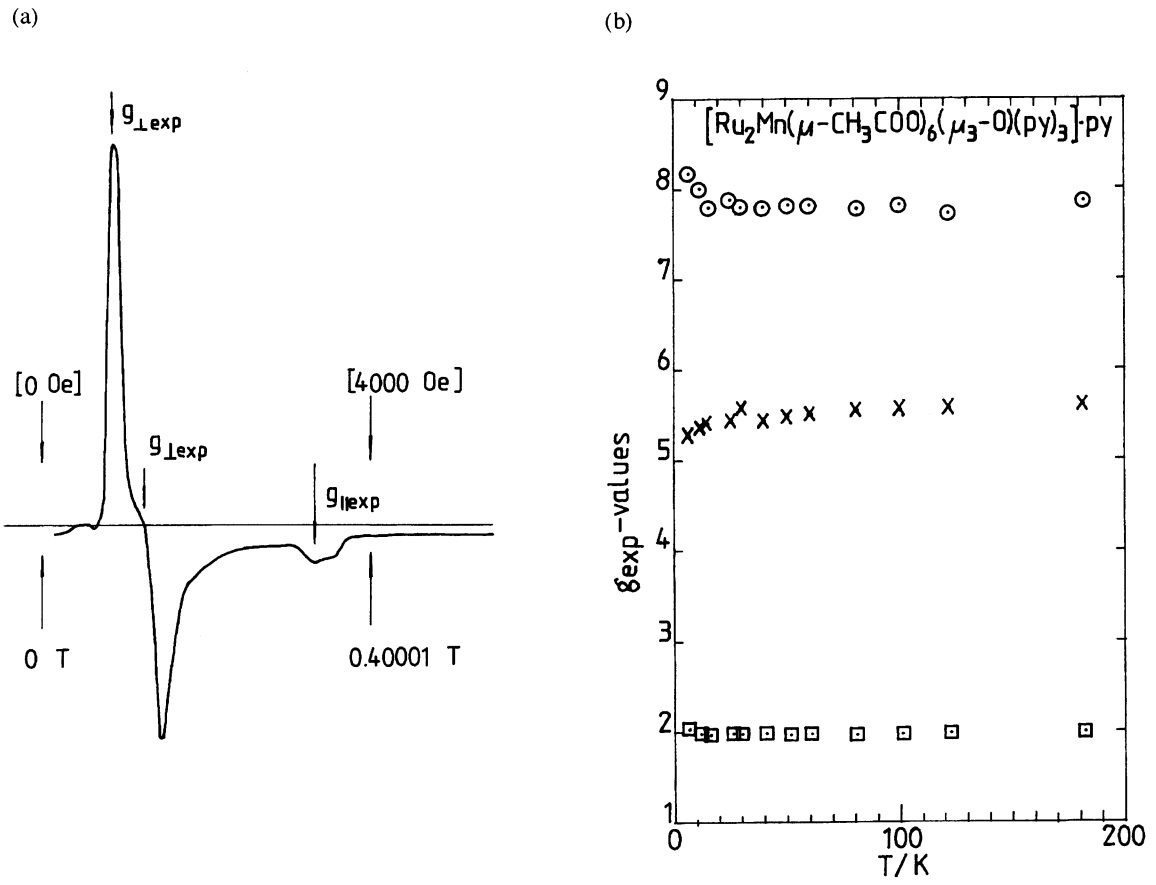

Fig. 4. (a) EPR of [$Ru_2Mn(\mu$-$CH_3COO)_6(\mu_3$-O)(py)$_3$]·py at 6.6 K as a function of the magnetic flux densities. 9.1675 GHz, 0.5±0.5 T, 16 min scan, 2 mW gain 10.0, and 100 kHz, 79.58 A m^{-1} mod. [ ] shows the applied magnetic field in the case of non-rationalized CGS emu. (b) Temperature dependences of experimental g-values, ⊙; $g_{\perp exp}$, ×; $g_{\perp exp}$, and ⊡; $g_{\parallel exp}$, observed by X-band of EPR of [$Ru_2Mn(\mu$-$CH_3COO)_6(\mu_3$-O)(py)$_3$]·py.

$$\chi'_M = (N\mu_0\mu_B^2/kT)\sum_{n=1,2} P(J_n, \alpha_n)\{42(g_a)^2\exp(5J_n/kT) + 17.5(g_b)^2\exp(-2J_n/kT) + 5(g_c)^2\exp(-7J_n/kT) + 17.5(g_d)^2\exp(-2\alpha_n J_n/kT)\}/\{8\exp(5J_n/kT) + 6\exp(-2J_n/kT) + 4\exp(-7J_n/kT) + 6\exp(-2\alpha_n J_n/kT)\}$$

$$\chi_M = \chi'_M + \chi_{TIPexp} + \chi_{dia} \quad (1)$$

Here J_n's are the superexchange interactions between M ion and Ru(III) and $\alpha_n J_n$'s are those between two Ru(III) ions, which act with each probability $P(J_n,\alpha_n)$, and $g_i = g_M + (g_M - g_{Ru})\{-S'(S'+1) - (S_2+S_3)(S_2+S_3+1) + S_1(S_1+1)\}/2S'(S'+1)$ is the g-value of each level of spins referring to Ref. 11, that is, $g_a = 0.714g_{Mn} + 0.286g_{Ru} = 2.15$, $g_b = 0.886g_{Mn} + 0.114g_{Ru} = 2.17$, $g_c = 1.400g_{Mn} - 0.400g_{Ru} = 2.22$, and $g_d = g_{Mn} = 2.18$.

To explain the molar magnetic susceptibility, strong antiferromagnetic exchange interactions J_1 and $\alpha_1 J_1$ through μ_3-O and weaker antiferromagnetic exchange interactions J_2 and $\alpha_2 J_2$ through μ-O–CCH_3–O were considered. In Fig. 3, one of the best fittings of the calculated effective Bohr magneton numbers, μ_{eff}'s, is shown by a broken line. The parameters of the broken line are $J_1/k = -300$ K, $\alpha_1 = -1$, $P(J_1,\alpha_1) = 0.425$, $J_2/k = -0.6$ K, $\alpha_2 = 4$, and $P(J_2,\alpha_2) = 0.575$. Mn(II) of the high spin state does not make any contribution to χ_{TIP}, so the experimental $\chi_{TIPexp} = 1.26\times10^{-9}$ m^3 was considered to be due to two Ru(III) ions.

It is said that the large antiferromagnetic exchange interaction causes the relaxation time to become too short and makes it difficult to observe the EPR signals. Thus observed EPR signals of the samples were considered to be due to spins under the weaker exchange interactions. In (Ru_2MnO), the lowest spin state is of $g_d = g_{Mn}$, but the exchange energy levels are determined not only by J, but also by α. In this case of (Ru_2MnO), the lowest exchange interaction energy level is of $W_d = J_2$ ($3\alpha_2/2$) and $g_d = g_{Mn}$. The signal of EPR at the lowest observed temperature would be mixed with small amounts of g_c and g_b, but would be mainly that of g_d. The exchange interaction energy levels due to the weaker exchange interactions are distributed in the region about 8 K above the lowest level. In Fig. 4b, temperature dependences of experimental g-values, two $g_{\perp exp}$ and a $g_{\parallel exp}$ are shown. They show that the mixings of g_d, g_c, g_b, and g_a are completed at lower temperatures than about 15 K.

$[Ru_2Fe(\mu\text{-}CH_3COO)_6(\mu_3\text{-}O)(py)_3]PF_6$. A molar magnetic susceptibility χ''_M of dark violet powder of (Ru_2FeO), which is corrected for χ_{dia}[15] $= -6.1480\times10^{-9}$ m^3 [-489.24×10^{-6} cm^3], increased with decreasing temperatures to near 2 K. From the graph of χ''_M versus reciprocal temperatures, χ_{TIPexp} of ca. 20.10×10^{-9} m^3 [ca. 1600×10^{-6} cm^3] was obtained. The experimental μ_{eff}'s calculated as a function of temperature, which were corrected for the experimental χ_{TIPexp} and χ_{dia}, are shown in Fig. 5, and in Fig. 1b by × marks. At room temperatures, μ_{eff}'s are about 5. Ru(III) in these clusters is assumed to be in the $^2T_{2g}$ state. The state of Fe(III) cannot be determined by these experimental μ_{eff}'s. Observed EPR signals by X-band were very anisotropic, as seen in Fig. 6. If Fe(III) is in a high spin state, the g-value should not be so anisotropic; here the observed signals are assumed mainly of the g-values of Fe(III). Then following Ref. 16, it was considered that very strong axial coordination field is working on Fe(III) in (Ru_2FeO), and EPR has also been observed by Q-band, giving $g_{\perp exp.\ averaged} = 5.90$. Using EPR in the two frequencies, g-values of Fe(III) were determined as $g_{\parallel} = 1.948$ and $g_{\perp} = 1.982$ with $|D| = 3.080\times10^{-2}$ m^{-1} [3.080 cm^{-1}]. In the following, the magnetic properties are analyzed for two low spin state Ru(III) ions of $g = 2.09$ and a high spin $^6A_{1g}$ state Fe(III) with averaged g-value=1.97.

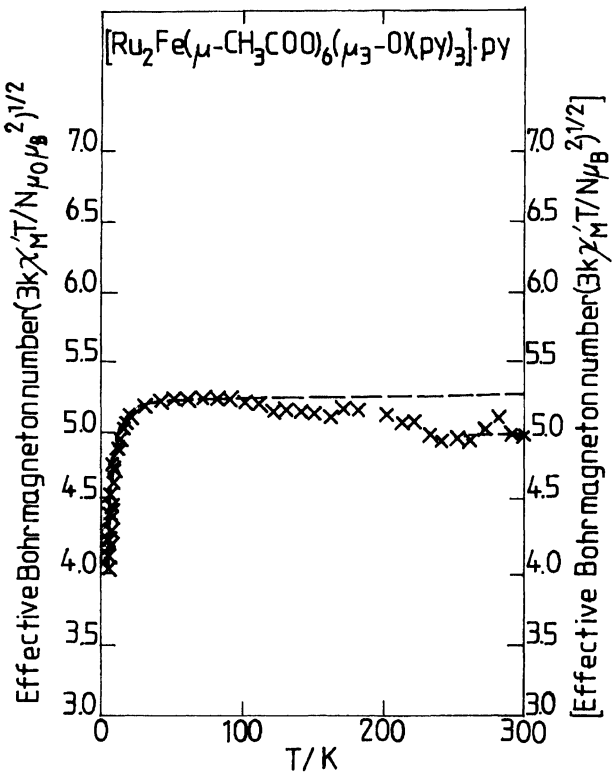

Fig. 5. Effective Bohr magneton numbers, μ_{eff}'s, of [Ru_2Fe-(μ-$CH_3COO)_6$(μ_3-O)$(py)_3$]·py as a function of temperatures. ×; data. χ_M's are corrected for χ_{TIPexp} and χ_{dia}. - - -; calculated values with $J_1/k = -300$ K, $\alpha_1 = -1$, $P(J_1,\alpha_1) = 0.480$, $J_2/k = -0.8$ K, $\alpha_2 = -1$, and $P(J_2,\alpha_2) = 0.520$. At 300 K, $J_1/k = -300$ K, $\alpha_1 = -1$, $P(J_1,\alpha_1) = 0.550$, $J_2/k = -0.8$ K, $\alpha_2 = -1$, and $P(J_2,\alpha_2) = 0.450$. $g_{Fe} = 1.97$ and $g_{Ru} = 2.09$.

As is known in the Hamiltonian[4,11] of the antiferromagnetic exchange interaction, the lowest spin state consists of an Fe(III) ion of $S = 5/2$. With increasing temperature the spin state changes to those including contributions of both Fe(III) and Ru(III). Namely, when S_1; spin of Fe(III) and $S_2 = S_3$; spins of Ru(III) are used, the spin states $W(S',S^*)$ are W_a (7/2,1), W_b (5/2,1), W_c (3/2,1), and W_d (5/2,0) respectively.

The calculated molar magnetic susceptibility[4,11] is the same with the formula (1), where g_a[11] $= 0.714g_{Fe} + 0.286g_{Ru} = 2.00$, $g_b = 0.886g_{Fe} + 0.114g_{Ru} = 1.983$, $g_c = 1.400g_{Fe} - 0.400g_{Ru} = 1.92$, and $g_d = g_{Fe} = 1.97$. The best fitted values shown by the broken line in Fig. 6 were at lower temperatures: $J_1/k = -300$ K, $\alpha_1 = -1$, $P(J_1,\alpha_1) = 0.480$, $J_2/k = -0.8$

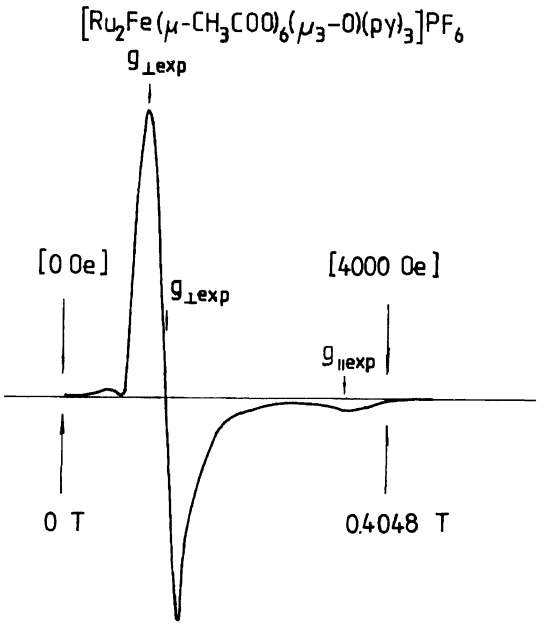

Fig. 6. EPR of $[Ru_2Fe(\mu\text{-}CH_3COO)_6(\mu_3\text{-}O)(py)_3]PF_6$ at 3.5—3.6 K as a function of the magnetic flux densities. 9.233625 GHz, 0.5±0.5 T, 2 mW gain 4.0×10^2 and 100 kHz, 1273 A m^{-1} mod. [ ] shows applied magnetic field in the case of non-rationalized CGS emu.

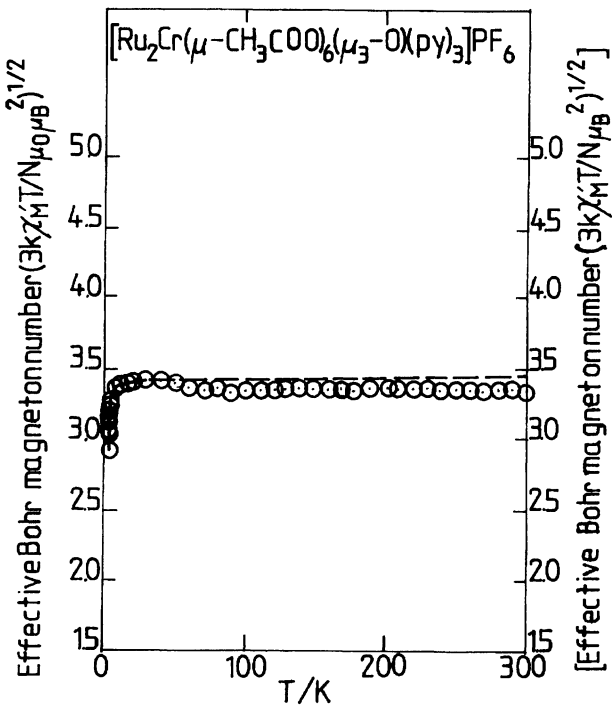

Fig. 8. Effective Bohr magneton numbers, μ_{eff}'s, of $[Ru_2Cr(\mu\text{-}CH_3COO)_6(\mu_3\text{-}O)(py)_3]PF_6$ as a function of temperatures. ⊙; data. χ'_M's are corrected for χ_{TIPexp} and χ_{dia}. ———; calculated values with $J_1/k=-450$ K, $\alpha_1=-1$, $P(J_1,\alpha_1)=0.520$, $J_2/k=-0.3$ K, $\alpha_2=-2$, and $P(J_2,\alpha_2)=0.480$. $g_{Cr}=2.00$ and $g_{Ru}=2.09$.

K, $\alpha_2=-1$, and $P(J_2,\alpha_2)=0.520$, and at 300 K, $J_1/k=-300$ K, $\alpha_1=-1$, $P(J_1,\alpha_1)=0.550$, $J_2/k=-0.8$ K, $\alpha_2=-1$, and $P(J_2,\alpha_2)=0.450$. Between 60 K and room temperatures, data show some fluctuations which seem due to some small distortions of the cluster from the fitting calculations.

In the case of (Ru_2FeO), the lowest exchange interaction energy state is of $W_c=J(7-\alpha/2)$ and $g_c=1.400g_{Fe}-0.400g_{Ru}=1.92$, which is a few Kelvin lower than that of $g_d=g_{Fe}$. In the EPR signal observed at 3.55 K, the effect of the mixing of g_c and g_d, and g_a and g_b as well could not be discriminated. In the EPR of X-band observed at temperatures 3.5—68 K, the pattern of signals showed no change, which seems to show that the mixings of the g-values of the weak exchange interaction energy levels are completed at lower temperatures than 3.5 K.

$[Ru_2Cr(\mu\text{-}CH_3COO)_6(\mu_3\text{-}O)(py)_3]RF_6$. The observed molar magnetic susceptibility of (Ru_2CrO) is shown in Fig. 7, where χ_{dia}[15]$=-5.5754\times10^{-9}$ m^3 [-443.68×10^{-6} cm^3] is removed. From this data, the χ_{TIP} was graphically obtained as 12.57×10^{-9} m^3 [1000×10^{-6} cm^3]. In Fig. 8 experimental μ_{eff}'s as a function of temperature are shown by ⊙ marks, where χ_{TIPexp} and χ_{dia} are corrected.

Observed EPR at 6.5 K is shown in Fig. 9a. This seems to have characteristic properties of Cr(III) ion in the strong axial anisotropic coordination field.[17] By Kambe's method,[4,11] the spin states $W(S',S^*)$, where S_1; spin of Cr(III) and $S_2=S_3$; spins of Ru(III), are $W_a(5/2,1)$, $W_b(3/2,1)$, $W_c(1/2,1)$, and $W_d(3/2,0)$. The lowest spin state is W_d under the assumption of the antiferromagnetic exchange interactions, and its g-value[11] is $g_d=g_{Cr}$. In the EPR signals of Fig. 9a, if they are assumed to be mainly due to g_{Cr}, the absorption at 0.1910 T is considered due to $|g\mu_BB-2D|$ and the absorption at 0.3275 T is considered due to $|-g\mu_BB|$. These gave $g_d=g_{Cr}=2.00$ and strength of the axial coordination field $|D|=0.24\times10^{-2}$m^{-1} [0.24 cm^{-1}]. EPRs were observed at temperatures between

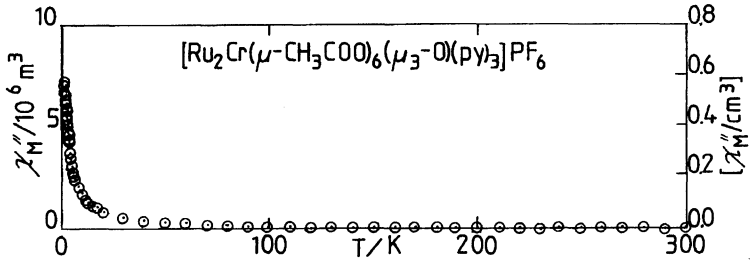

Fig. 7. The molar magnetic susceptibility of $[Ru_2Cr(\mu\text{-}CH_3COO)_6(\mu_3\text{-}O)(py)_3]PF_6$ as a function of temperatures. χ''_M's are corrected for χ_{dia}.

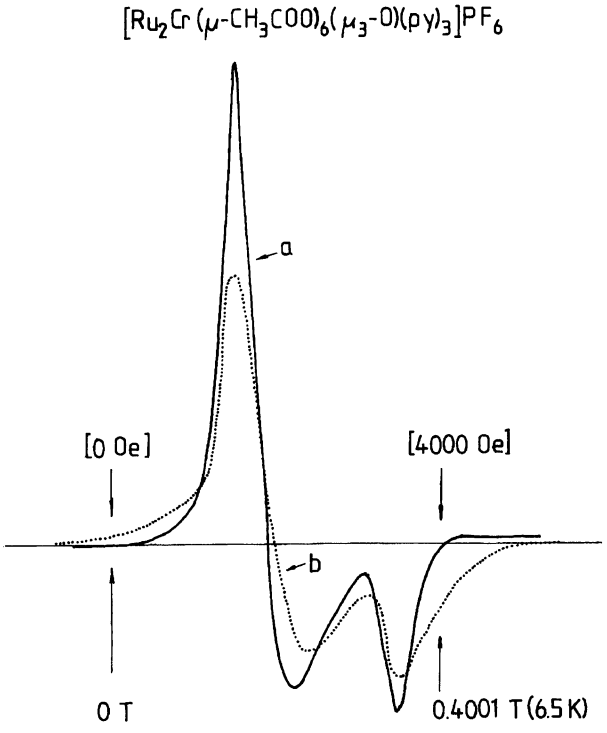

Fig. 9. EPR of $[Ru_2Cr(\mu\text{-}CH_3COO)_6(\mu_3\text{-}O)(py)_3]PF_6$. a: At 6.5 K, 9.16301 GHz, 0.5±0.5 T, 16 min, 10 mW, gain 2.2×10, and 100 kHz, 1273.2 A m^{-1} mod. b: At 144.8 K, 9.2065 GHz, 0.3±0.25 T, 8 min, 10 mW, gain 3.2×100, and 100 kHz, 795.8 A m^{-1} mod. [ ] shows applied magnetic field in the case of the non-rationalized CGS emu.

6.5 K and room temperature. The signals at 145 K are shown in Fig. 9b, which have changed by g_a, g_b, and g_c with temperatures. The signal assigned to g_{Cr} was considered to be almost temperature independent. The g-value of Ru(III) could not be determined from the EPR data, but as for other samples $g_{Ru}=2.09$ was used.

The molar magnetic susceptibility of (Ru_2CrO) was calculated[4,11] using

$$\chi_M' = (N\mu_O\mu_B^2/kT)\sum_{n=1,2} P(J_n,\alpha_n)\{17.5(g_a)^2\exp(3J_n/kT) + 5(g_b)^2\exp(-2J_n/kT) + 0.5(g_c)^2\exp(-5J_n/kT) + 5(g_d)^2\exp(-2\alpha_n J_n/kT)\}/\{6\exp(3J_n/kT) + 4\exp(-2J_n/kT) + 2\exp(-5J_n/kT) + 4\exp(-2\alpha_n J_n/kT)\}$$

$$\chi_M = \chi_M' + \chi_{TIP} + \chi_{dia} \quad (2)$$

where g_a[11] $= 0.600g_{Cr} + 0.400g_{Ru} = 2.04$, $g_b = 0.733g_{Cr} + 0.267g_{Ru} = 2.02$, $g_c = 1.667g_{Cr} - 0.667g_{Ru} = 1.94$, and $g_d = g_{Cr} = 2.00$. The two exchange interactions through μ_3-O and μ-CH_3COO will work with each probability $P(J_n,\alpha_n)$. In the case of the symmetrical $[Ru_3(\mu\text{-}CH_3COO)_6(\mu_3\text{-}O)(py)_3]ClO_4$,[7] the result of the fitting showed that the probability of the exchange interactions through μ-CH_3COO paths was zero. The calculated μ_{eff}'s are shown with a broken line in Fig. 8, where fitted parameters were $J_1/k=-450$ K, $\alpha_1=-1$, $P(J_1,\alpha_1)=0.520$, and $J_2/k=-0.3$ K, $\alpha_2=-2$, and $P(J_2,\alpha_2)=0.480$. In this case, the lowest exchange interaction energy level is $W_c=J(5-\alpha/2)$. As $J_2/k=-0.3$ K is small, $W_a=-J(3+\alpha/2)=0.6$ K, $W_b=J(2-\alpha/2)=-0.9$ K, $W_c=-1.8$ K, and $W_d=J(3\alpha/2)=0.9$ K. When W_c is considered to be the lowest, W_b, W_a, and W_d are at 0.9, 2.4, and 2.7 K higher levels respectively. In the signals observed in Fig. 9a, there is mixing of g_a, g_b, and g_d. But the characteristic of Cr(III) is strongly seen in the observation, because g_a, g_b, and g_d have more proportions of Cr(III) than of Ru(III), as seen in the above. The signal patterns of Fig. 9a did not show any changes with temperatures to near 120 K.

$[Ru_2Ni(\mu\text{-}CH_3COO)_6(\mu_3\text{-}O)(py)_3]\cdot py$ and $[Ru_2Ni(\mu\text{-}CH_3COO)_6(\mu_3\text{-}O)(py)_3]\cdot CH_2Cl_2$. $[Ru_2Ni(\mu\text{-}CH_3COO)_6(\mu_3\text{-}O)(py)_3]\cdot CH_2Cl_2$ was synthesized for EPR. The observed molar magnetic susceptibilities, corrected for each χ_{dia},[15] -5.9062×10^{-9} m^3 [-471.00×10^{-6} cm^3] or -5.4774×10^{-9} m^3 [-435.88×10^{-6} cm^3], were about 62.8×10^{-9} m^3 [5000×10^{-6} cm^3] at room temperature. The observed molar magnetic susceptibilities versus reciprocal temperatures curve gave the χ_{TIPexp} of 11.3×10^{-9} m^3 [ca. 900×10^{-6} cm^3] for the former and 10.1×10^{-9} m^3 [ca. 800×10^{-6} cm^3] for the latter. The experimental molar magnetic susceptibility corrected for χ_{dia} and χ_{TIPexp} was fitted by the calculated molar magnetic susceptibility followed Kambe's spin vector model[4,11] to see the superexchange interactions among a Ni(II) and two Ru(III) in the triangular trinuclear cluster. The calculated molar magnetic susceptibility is

$$\chi_M' = (N\mu_O\mu_B^2/kT)\sum_{n=1,2} P(J_n,\alpha_n)\{10(g_a)^2\exp(2J_n/kT) + 2(g_b)^2\exp(-2J_n/kT) + 2(g_d)^2\exp(-2J_n\alpha_n/kT)\}/\{5\exp(2J_n/kT) + 3\exp(-2J_n/kT) + \exp(-4J_n/kT) + 3\exp(-2J_n\alpha_n/kT)\}$$

$$\chi_M = \chi_M' + \chi_{TIP} + \chi_{dia} \quad (3)$$

The spin states under antiferromagnetic exchange interactions are $W_a(2,1)$, $W_b(1,1)$, $W_c(0,1)$, and $W_d(1,0)$, where S_1 is a spin of Ni(II) and S_2 and S_3 are spins of two Ru(III). The calculated g-values are $g_a=0.500g_{Ni}+0.500g_{Ru}$, $g_b=0.500g_{Ni}+0.500g_{Ru}$, and $g_d=g_{Ni}$.

The EPR of $[Ru_2Ni(\mu\text{-}CH_3COO)_6(\mu_3\text{-}O)(py)_3]\cdot CH_2Cl_2$ gave complex signals, as shown in Fig. 10, which were considered to be mixed signals. A part of the signals appears stronger at lower temperatures, as seen in Fig. 10a, which gave $g_1=2.636$, $g_2=2.357$, and $g_3=1.970$, that is, $g_{averaged}=2.34$. This $g_{av.}=2.34$ was considered to be the g-value of the Ni(II) in the lowest state W_d; the calculated g-values were $g_a=g_b=2.22$ and $g_d=2.34$. One of the best fitted values of the experimental molar magnetic susceptibility of (Ru_2NiO) was $J_1/k=-300$ K, $\alpha_1=1.995$, $P(J_1,\alpha_1)=0.745$, $J_2/k=-140$ K, $\alpha_2=3.00$, and $P(J_2,\alpha_2)=0.255$, which is shown in Fig. 11 with the broken line, where + marks are the observed values corrected for χ_{TIPexp} and χ_{dia}. The g_d is the g-value of the lowest exchange interaction energy state $W_d=J(4\alpha)$ and should correspond to that of the g-value observed in EPR at the lowest temperature. The residual signals of EPR, Fig. 10b, drawn with a dotted line, seem stronger at

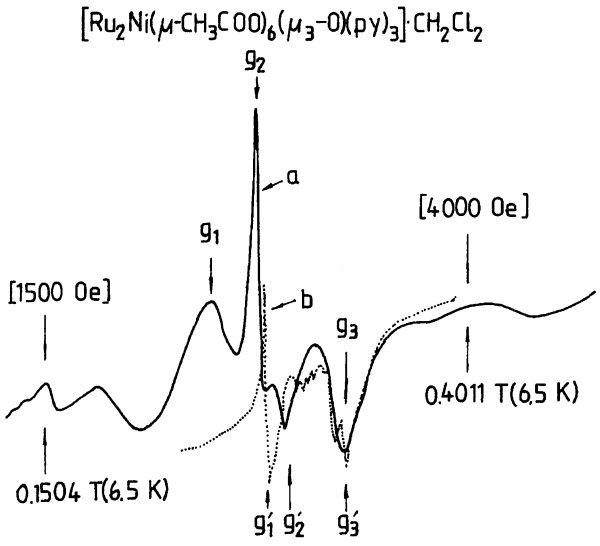

Fig. 10. EPR of $[Ru_2Ni(\mu\text{-}CH_3COO)_6(\mu_3\text{-}O)(py)_3]\cdot CH_2Cl_2$ as a function of the magnetic flux densities. a: At 6.5 K, 9.1627 GHz, 0.5±0.5 T, 16 min, 10 mW, gain 6.3×10^3, and 100 kHz, 1273.24 A m^{-1} mod. b: At 114 K, 9.207 GHz, 0.3±0.25 T, 16 min, 10 mW, gain 3.2×10^3, and 100 kHz, 795.8 A m^{-1} mod. [ ] shows the applied magnetic field in the case of the non-rationalized CGS emu.

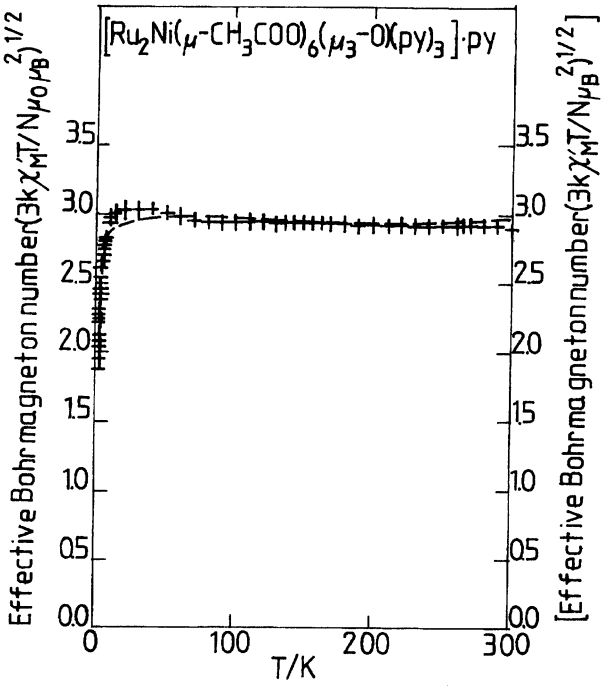

Fig. 11. Effective Bohr magneton numbers, μ_{eff}'s, of $[Ru_2Ni(\mu\text{-}CH_3COO)_6(\mu_3\text{-}O)(py)_3]\cdot py$ as a function of temperatures. +; data. χ_M''s are corrected for χ_{TIPexp} and χ_{dia}. ---; calculated values with $J_1/k=-300$ K, $\alpha_1=1.995$, $P(J_1,\alpha_1)=0.745$, $J_2/k=-140$ K, $\alpha_2=3.00$, and $P(J_2,\alpha_2)=0.255$. $g_{Ni}=2.34$ and $g_{Ru}=2.09$

near 110 K; these are $g_1'=2.352$, $g_2'=2.233$, and $g_3'=1.997$, that is $g_{av.}=2.20$. This signal was considered to be the mixture of g_d, g_b, and g_a, at the higher temperatures.

$[Ru_2Co(\mu\text{-}CH_3COO)_6(\mu_3\text{-}O)(py)_3]\cdot py$. Experimental molar magnetic susceptibility of (Ru_2CoO), which is corrected for χ_{dia}[15] of -5.9439×10^{-9} m^3 [-473.00×10^{-6} cm^3], is about 37.7×10^{-9} m^3 [3000×10^{-6} cm^3] at room temperature, which is smaller than that of (Ru_2NiO). The (Ru_2NiO) is considered to be the state which consists of two Ru(III) with $S=1/2$ and Ni(II) with $S=1$; then Co(II) in the (Ru_2CoO) has been considered to be in the state that consists of two Ru(III) with $S=1/2$ and Co(II) with $S=1/2$ (Fig. 1b). EPR experiments have given g-values[11] of $g_1=5.7$—6.05, $g_2=4.2$—4.3, and $g_3=3.0$—3.15, namely, $\sum_i g_i=12.9$—13.5 with fluctuations in the temperature region lower than 80 K, as seen in Fig. 12. Referring to Refs. 18, 19, and 20, in the present paper, Co(II) in (Ru_2CoO) is assumed to be in the low spin state of $S=1/2$.

The experimental molar magnetic susceptibility versus reciprocal temperature curve gave about 36.2×10^{-9} m^3 [288×10^{-6} cm^3] at $T^{-1}=0$ K^{-1}, which shows that χ_{TIP} is 36.2×10^{-9} m^3. To find the superexchange interactions acting in the (Ru_2CoO) cluster, the experimental molar magnetic susceptibility corrected for χ_{dia} and $\chi_{TIPexp}=36.2\times10^{-9}$ m^3 was used. The μ_{eff} calculation was tried using this susceptibility. The molar magnetic susceptibility under the spin vector model was calculated following Kambe's method.[4,11] The formula for (Ru_2CoO) is

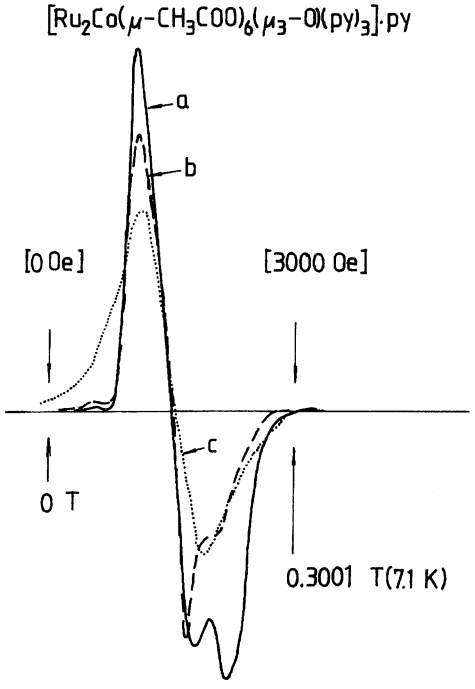

Fig. 12. EPR of $[Ru_2Co(\mu\text{-}CH_3COO)_6(\mu_3\text{-}O)(py)_3]\cdot py$ as a function of the magnetic flux densities. a: At 7.1 K, 9.17413 GHz, 0.5±0.5 T, 2 mW, gain 1.6×10, and 100 kHz, 79.58 A m^{-1} mod. b: At 82.6 K, 9.17408 GHz, 0.5±0.5 T, 10 min, gain 3.2×10, and 100 kHz, 79.58 A m^{-1} mod. c: At 109.7 K, 9.17423 GHz, 0.5±0.5 T, 16 min, gain 8.0×10, and 100 kHz, 79.58 A m^{-1} mod. [ ] shows the applied magnetic field in the non-rationalized CGS emu.

$$\chi'_M = (N\mu_O\mu_B^2/4kT)\sum_{n=1,2} P(J_n,\alpha_n)\{10(g_a)^2\exp(J_n/kT) + (g_b)^2\exp(-2J_n/kT) + (g_c)^2\exp(-2\alpha_n J_n/kT)\} / \{2\exp(J_n/kT) + \exp(-2J_n/kT) + \exp(-2\alpha_n J_n/kT)\}$$

$$\chi_M = \chi'_M + \chi_{TIP} + \chi_{dia} \quad (4)$$

where $g_a = 0.333g_{Co} + 0.667g_{Ru}$, $g_b = -0.333g_{Co} + 1.333g_{Ru}$, and $g_c = g_{Co}$ following Ref. 11. As g-value of Co(II), an averaged value obtained by EPR (Fig. 12a) at temperatures lower than 80 K, that is, $g_{Co} = 4.55$ has been used. As the g-value of Ru(III), $g_{Ru} = 2.00$ has been assumed considering a stronger delocalization of spins. The spin states from the Hamiltonian are W_a (3/2,1), W_b (1/2,1), and W_c (1/2,0). The lowest spin state is that of $g_c = g_{Co}$. After several fittings were tried, it has been found that, if 36.2×10^{-9} m^3 is assumed as χ_{TIP}, the fitting is impossible. The lowest electronic absorption in Fig. 13 observed in the range between 5×10^6 m^{-1} [50000 cm^{-1}] and 1.176×10^6 m^{-1} [11760 cm^{-1}] was at 1.7590×10^6 m^{-1} [17590 cm^{-1}]. If we assume that this absorption, Δ, is due to an electronic transition among terms separated by the axial anisotropic low symmetric ligand field of Co(II) and referring to Ref. 21, we can get $\chi_{TIPexp} = 4N\mu_O\mu_B^2/\Delta = 0.754\times10^{-9}$ m^3 [59.4×10^{-6} cm^3] for Co(II). For χ_{TIP} due to Ru(III), 5.03×10^{-9} m^3 [ca. 400×10^{-6} cm^3] is assumed considering Ref. 22. Instead of $\chi_{TIPexp} = 36.19\times10^{-9}$ m^3 [2880×10^{-6} cm^3], here we use 10.8×10^{-9} m^3, namely, $\chi_{TIP} = 0.754\times10^{-9}$ m^3 + $2\times5.03\times10^{-9}$ m^3 [60×10^{-6} cm^3 + $2\times400\times10^{-6}$ cm^3 = 860×10^{-6} cm^3]. The μ_{eff}'s of (Ru_2CoO) corrected for χ_{dia} and $\chi_{TIP} = 10.8\times10^{-9}$ m^3 as a function of temperature are shown in Fig. 14 with ⊡ marks.

One of the best fittings of Eq. 4 was $J_1/k = -300$ K, $\alpha_1 = -2$, $P(J_1,\alpha_1) = 0.839$, $J_2/k = -50$ K, $\alpha_2 = -2$, and $P(J_2,\alpha_2) = 0.161$, where $g_a = 2.85$, $g_b = 1.15$, $g_c = g_{Co} = 4.55$, and $g_{Ru} = 2.00$. This is shown in Fig. 14 with a broken line. But to find a good fitting at lower temperatures than 20 K was impossible without antiferromagnetic interactions among clusters. The calculation plotted in Fig. 14 assumed the antiferromagnetism of $\theta = -2.0$ K. The lowest exchange interaction level is that

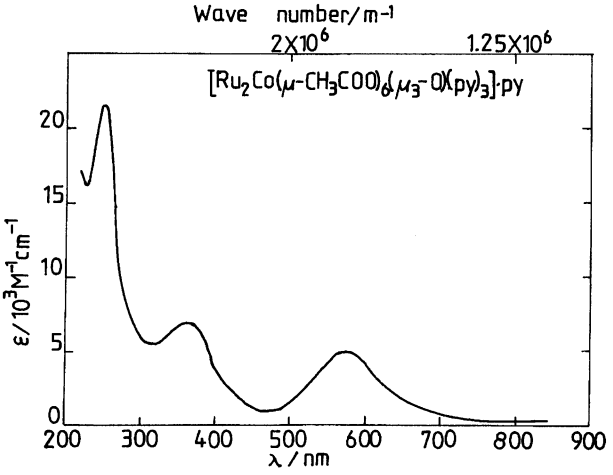

Fig. 13. Electronic absorption of $[Ru_2Co(\mu\text{-}CH_3COO)_6(\mu_3\text{-}O)(py)_3]\cdot py\cdot CH_3CN$ soln.

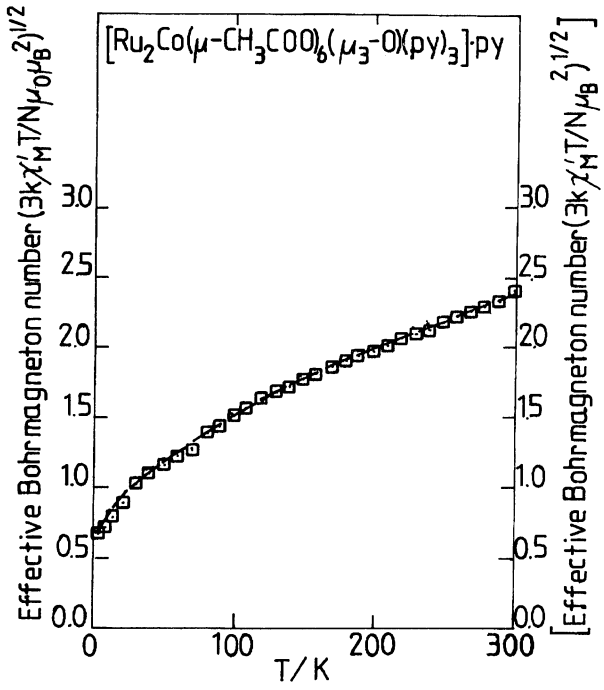

Fig. 14. Effective Bohr magneton number, μ_{eff}'s, of $[Ru_2Co(\mu\text{-}CH_3COO)_6(\mu_3\text{-}O)(py)_3]\cdot py$ as a function of temperatures. ⊡; data. χ'_M's are corrected for χ_{TIP} and χ_{dia}. - - -; calculated values with $J_1/k = -300$ K, $\alpha_1 = -2$, $P(J_1,\alpha_1) = 0.839$, $J_2/k = -50$ K, $\alpha_2 = -2$, $P(J_2,\alpha_2) = 0.161$. $g_{Co} = 4.55$ and $g_{Ru} = 2.00$, and antiferromagnetic $\theta = -2.0$K.

of $W_b = J(2-\alpha/2)$ of g_b, but EPR due to $g_b = 1.15$ should be found at higher applied magnetic field. Then the observed signal around 0.15—0.2 T at 7.1—7.2 K was considered to be of the level, mainly, of g-value of Co(II), namely g_{Co}. The EPR signals of g-value very slowly changed to 80 K (Fig. 12b) and at 110 K (Fig. 12c) fairly changed signals were observed. The observed g_{Co} at 7 K was of $g_1 = 5.9$, $g_2 = 4.3$, and $g_3 = 3.1$ showing low symmetric ligand field.

Summary

In Kambe's vector model[4] only the isotropic exchange interactions in the spin Hamiltonian[5,6,23] are considered. This is due to that the anisotropic part of the symmetric exchange interaction through space becomes negligibly small when the spin–orbit interaction becomes smaller. The antisymmetric part of the exchange interaction, which produces the weak ferromagnetism, is also neglected in the calculation because the experiments showed no weak ferromagnetism in any of the samples.

Results of the above fitting calculations to find the exchange interactions in the clusters showed that the magnitude of the main superexchange interaction between a Ru(III) ion and the M ion was $J_1/k = -300$ K in almost all the samples. The spin states under antiferromagnetic exchange interactions within the cluster are determined with $S' = S_1 + S_2 + S_3$ and $S^* = S_2 + S_3$. The exchange interaction energy states depend not only on J but also α. In (Ru_2MnO) and (Ru_2NiO), the lowest exchange interaction energy states were of the

lowest spin states and those of g_{Mn} and g_{Ni} respectively. In (Ru_2FeO), the lowest exchange interaction energy level was of $g_c=1.400g_{Fe}-0.400g_{Ru}$ and the level of $g_d=g_{Fe}$ was ca 7 K above of it. Though mixing of g_{Ru} in the signal at the lowest observed temperature could not be discriminated, the signal was considered to have the characteristic of g_{Fe}. (Ru_2CrO) also had a similar effect on the EPR signal at the lowest observed temperature. In the case of (Ru_2CoO) fitting had many difficulties, but the EPR signal of $g_{av.}=4.55$ was considered to be due to Co(II) ion.

In the case of (Ru_2CoO), one needed to take $g_{Ru}=2.00$, that is, a g-value of only a spin. The molecular orbital due to μ_3-O between Ru(III) ions was considered that induced delocalization of electrons. This effect might exist in other clusters, not only in the case of (Ru_2CoO). The calculations of magnetic properties in the molecular orbitals should be progressed.

In Ref. 24, Dr. T.-Y. Dong and co-workers have reported "Magnetic and Spectral Properties of Heterotrinuclear Acetates $[Ru_2Co(\mu_3\text{-}O)(\mu\text{-}CH_3CO_2)_6(py)_3]^{n+}$ (n=0 or 1)". Their sample of n=0 has the same coordination as our (Ru_2CoO), but their compound shows the spin of 3/2 of Co.

The authors deeply thank Professor Kazuaki Fukamichi, Faculty of Engineering, Tohoku University and Professor Emeritus Yasuaki Nakagawa, Tohoku University, for their encouragements. One of the authors, H. K. thanks Professor Yoshitami Ajiro, Department of Physics, Kyushu University, and Professor Dr. Yurii V. Yablokov, Kazan Physical Technical Institute, Tatarstan, Russia, for the detailed discussions of the results of the EPR experiments. She thanks Dr. Haruo Akashi, Okayama University of Science, for his kind cooperation with the experiments.

References

1) J. H. Van Vleck, "The Theory of Electric and Magnetic Susceptibilities," Oxford University Press, London (1932).

2) R. J. Myers, "Molecular Magnetism and Magnetic Resonance Spectroscopy," Prentice-Hall Inc., Englewood Cliffs, New Jersey (1973).

3) "Theory and Applications of Molecular Paramagnetism," ed by E. A. Boudreaux and L. N. Mulay, John Wiley & Sons, New York, London, Sydney, and Toronto (1976).

4) K. Kambe, *J. Phys. Soc. Jpn.*, **5**, 48 (1950).

5) "Magneto-Structural Correlations in Exchange Coupled Systems," ed by R. D. Willett, D. Gatteschi, and O. Kahn, D. Reidel Publishing Company, Dordrecht, Boston, Lancaster (1985).

6) A. Bencini and D. Gatteschi, "Electron Paramagnetic Resonance of Exchange Coupled Systems," Springer-Verlag, Berlin, Heidelberg, New York, London, Paris, Tokyo, and Hong Kong (1990).

7) H. Kobayashi, N. Uryû, A. Tokiwa, T. Yamaguchi, Y. Sasaki, and T. Ito, *Bull. Chem. Soc. Jpn.*, **65**, 198 (1992).

8) T.Głowiak, M. Kubiak, and T. Szymańska-Buzar, *Acta Crystallogr., Sect. B.*, **33**, 1732 (1979).

9) H. Kobayashi, N. Uryû, I. Mogi, R. Miyamoto, Y. Ohba, M. Iwaizumi, Y. Sasaki, A. Ohto, and T. Ito, *Bull. Chem. Soc. Jpn.*, **68**, 2551 (1995).

10) B. I. Bleaney and B. Bleaney, "Electricity and Magnetism," 3rd ed, Oxford University Press.

11) L. C. W. Baker, V. E. S. Baker, S. H. Wasfi, G. A. Candela, and A. H. Kahn, *J. Chem. Phys.*, **56**, 4917 (1972); Yu. V. Yablokov, V. A. Gaponenko, M. V. Eremin, V. V. Zelentsov, and T. A. Zhemchuzhnikova, *Sov. Phys.-JETP*, **38**, 988 (1974); В. К. ВОРОНКОВА, Л. В. МОСИНА, Ю. В. ЯБЛОКОВ, Ш. Х. АБДУЛЛАЕВ, В. В. ЗЕЛЕНЦОВ, Т. А. НАСОНОВА, ИХ. М. ЯКУЪОВ, "ЖУРНАЛ НЕОРГАНИЧЕСКОЙ ХИМИИ," Том 33, 1487 (1988); and G. V. Kokoszka and R. W. Duerst, *Cood. Chem. Rev.*, **5**, 209 (1970).

12) A. Ohto, Y. Sasaki, and T. Ito, *Inorg. Chem.*, **33**, 1245 (1994).

13) Y. Sasaki, Y. Yoshida, A. Ohto, A. Tokiwa, T. Ito, H. Kobayashi, N. Uryû, and I. Mogi, *Chem. Lett.*, **1993**, 69; A. Ohto, PhD. Thesis, 1995.

14) "Manual of Symbols and Terminology for Physico-Chemical Quantities and Units," IUPAC, Pergamon Press, 1979 and NBS Guide-lines for Use of the Magnetic System NBS 1977.

15) R. R. Gupta, "Landolt-Börnstein, Numerical Data and Functional Relationships in Science and Technology," New Series II/16, ed by K.-H. Hellwege and A. M. Hellewege.

16) E. S. Kirkpatrick, K. A. Müller, and R. S. Rubins, *Phys. Rev.*, **135**, A86 (1964).

17) L. S. Singer, *J. Chem. Phys.*, **23**, 379 (1955).

18) B. N. Figgis, "Introduction to Ligand Fields," Interscience Publishers, a division of John Wiley and Sons, New York, London, Sydney.

19) A. Abragam and M. H. L. Pryce, *Proc. R. Soc. (London) A*, **206**, 173 (1951); B. Bleaney and D. J. E. Ingram, *Proc. R. Soc. (London), A*, **208**, 143 (1951).

20) B. Bleaney, *Physica*, **XVII**, 175 (1951).

21) J. J. Ziółkowski, F. Pruchnik, and T. Szymanska-Buzar, *Inorg. Chim. Acta*, **7**, 473 (1973); N. Fogel, C. C. Lin, C. Ford, and W. Grindstaff, *Inorg. Chem.*, **3**, 720 (1964).

22) J. M. Fletcher, W. E. Gardner, A. C. Fox, and G. Topping, *J. Chem. Soc. A*, **1967**, 1038.

23) B. Bleaney, F. R. S., and K. D. Bowers, *Proc. R. Soc. (London) A*, **214**, 451 (1952); T. Moriya, *Phys. Rev.*, **120**, 91 (1960).

24) T.-Y. Dong, H.-S. Lee, T.-Y. Lee, and C.-F. Hsieh, *J. Chin. Chem. Soc.*, **39**, 393 (1992).